Synthesis, biological evaluation and molecular modeling study of some new methoxylated 2-benzylthio-quinazoline-4(3H)-ones as nonclassical antifolates

Shahenda M. El-Messery, Ghada S. Hassan, Mahmoud N. Nagi, El-Sayed E. Habib, Sarah T. Al-Rashood, Hussein I. El-Subbagh

PII: S0960-894X(16)30843-5
DOI: http://dx.doi.org/10.1016/j.bmcl.2016.08.022
Reference: BMCL 24148

To appear in: *Bioorganic & Medicinal Chemistry Letters*

Received Date: 2 June 2016
Revised Date: 1 August 2016
Accepted Date: 9 August 2016

Please cite this article as: El-Messery, S.M., Hassan, G.S., Nagi, M.N., Habib, E.E., Al-Rashood, S.T., El-Subbagh, H.I., Synthesis, biological evaluation and molecular modeling study of some new methoxylated 2-benzylthio-quinazoline-4(3H)-ones as nonclassical antifolates, *Bioorganic & Medicinal Chemistry Letters* (2016), doi: http://dx.doi.org/10.1016/j.bmcl.2016.08.022

Synthesis, biological evaluation and molecular modeling study of some new methoxylated 2-benzylthio-quinazoline-4(3H)-ones as nonclassical antifolates.

Shahenda M. El-Messery,[a*] Ghada S. Hassan,[b] Mahmoud N. Nagi,[c] El-Sayed E. Habib,[d,e] Sarah T. Al-Rashood,[f] Hussein I. El-Subbagh.[b,g*]

[a]*Department of Pharmaceutical Organic Chemistry, Faculty of Pharmacy, Mansoura University, P.O.Box 35516, Mansoura, Egypt.*

[b]*Department of Medicinal Chemistry, Faculty of Pharmacy, Mansoura University, P.O.Box 35516, Mansoura, Egypt.*

[c]*Department of Pharmacology, College of Pharmacy, King Saud University, Riyadh, 11451, Saudi Arabia.*

[d]*Department of Pharmaceutics and pharmaceutical technology (Microbiology), College of Pharmacy, Taibah University, Almadinah Almunawwarah, 344, Saudi Arabia*

[e]*Department of Microbiology, Faculty of Pharmacy, Mansoura University, P.O.Box 35516, Mansoura, Egypt*

[f]*Department of Pharmaceutical Chemistry, College of Pharmacy, King Saud University, P.O.Box 2457, Riyadh 11451, Saudi Arabia.*

[g]*Department of Pharmaceutical Chemistry, Faculty of Pharmaceutical Sciences & Pharmaceutical Industries, Future University, 12311 Cairo, Egypt.*

Abstract

A new series of 2,3,6-substituted-quinazolin-4-ones was designed, synthesized, and evaluated for their *in vitro* DHFR inhibition, antimicrobial, and antitumor activities. Compounds **28** and **61** proved to be active DHFR inhibitors with IC_{50} 0.02 and 0.01 μM, respectively. Molecular modeling studies concluded that recognition with the key amino acid Phe34 is essential for binding and hence DHFR inhibition. Compounds **34**, **56** and **66** showed broad spectrum antimicrobial activity comparable to Gentamicin and Ciprofloxacin. Compounds **40** and **64** showed broad spectrum antitumor activity toward several tumor cell lines and proved to be 10 fold more active than 5-FU, with GI_{50} MG-MID values of 2.2 and 2.4 μM, respectively.

Keywords: Synthesis, quinazolin-4-ones, DHFR inhibition, antimicrobial testing, antitumor screening, molecular modeling study.

Correspondence: Hussein I. El-Subbagh, Department of Medicinal Chemistry, Faculty of Pharmacy, Mansoura University, Mansoura 35516, Egypt
E-mail: subbagh@yahoo.com.
Tel: +20-50-2247800, **Fax**: +20-50-2247496

Shahenda M. El-Messery Department of Pharmaceutical Organic Chemistry, Faculty of Pharmacy, Mansoura University, Mansoura 35516, Egypt
E-mail: shahenda76@yahoo.com
Tel: +20-50-2247800**, Fax** +20-50-2247496

Dihydrofolate reductase (DHFR) enzyme has a crucial role in conjunction with thymidylate synthase (TS) in the reductive methylation of deoxyuridine monophosphate (dUMP) to deoxythymidine monophosphate (dTMP) utilizing N^5,N^{10}-methylene-tetrahydrofolate as a cofactor. Inhibition of DHFR or TS activity leads to "thymineless death" of the cell [1,2]. DHFR inhibition is an attractive goal for the developing of chemotherapeutic agents against bacterial and parasitic infections as well as cancer [3]. Previous studies conducted in our laboratories [4-22], especially what has been reported about the DHFR inhibition [17-19], allowed the allocation of certain pharmacophoric characteristics for the active quinazoline DHFR inhibitors. Bearing a basic nitrogen atom at *N*-1, a 4-carbonyl function, and hydrophobic π-system regions and their relative spatial distances are the major pharmacophoric requirements. The type of substitution, in addition to the spatial considerations of the π-systems in regard to the quinazoline nucleus manipulated the DHFR inhibition activity [17-19,22]. Compounds **A**-**C** (Figure 1) represent the active DHFR inhibitors obtained as a result of implementing these pharmacophoric features with IC_{50} range of 0.3-1.0 μM.

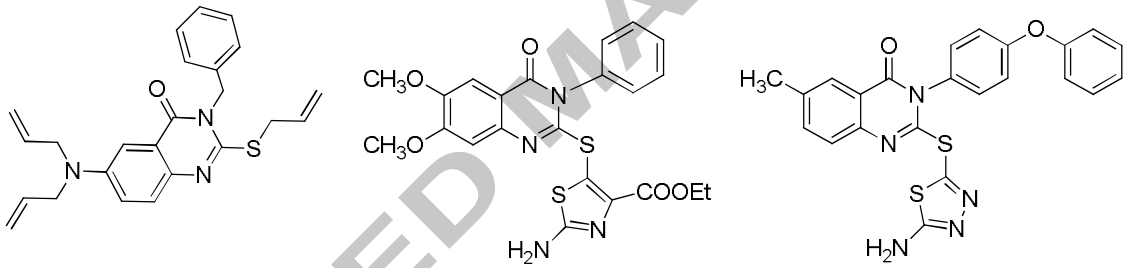

Figure 1: Structures of some literature antifolate lead compounds.

In continuation to our previous efforts, a new series of 2,3,6-substituted-quinazolin-4-ones was designed. The new analogues possess methoxylated 2-(arylmethylthio)- as hydrophobic π-system regions replacing the 2-heteroaryl functions reported earlier [22], as an attempt to explore the scope and limitations of activity of this class of compounds. In addition, 6-Chloro, 6-methyl, or 6,7-dimethoxy functions, were introduced representing electron donating and electron withdrawing substituents. Also, substituted phenyl or benzyl group were added to position 3- of the quinazolin-4-one nucleus as a realization of the pharmacophoric requirements of this class of DHFR inhibitors. Most of the function groups used in this design are known to contribute to DHFR inhibition activity [23,24]. The aim of this study is to locate novel synthetic lead compound(s), and its *in vitro* testing as DHFR inhibitors. As an application, the synthesized compounds were also tested against a panel of

standard strains of *Gram-positive* and *Gram-negative* bacteria; and screened for their *in-vitro* antitumor activity using the NCI's disease-oriented human cell lines assay [25-28].

The title compounds were prepared according to the synthetic strategy described in Schemes 1 and 2. The starting materials 6-methyl- (**4-9**), 6-chloro- (**10-15**), or 6,7-dimethoxy- (**16-21**) -3-(phenyl, 4-methoxyphenyl, 2-methoxyphenyl, 2,4-dimethoxyphenyl, 4-chlorophenyl or 4-methylphenyl)-quinazolin-4(*3H*)-one-2-thiones and the 6-methyl-, 6-chloro- or 6,7-dimethoxy-3-(benzyl)-quinazolin-4(*3H*)-one-2-thiones (**58-60**) were prepared adopting reported procedures [17-19,22]. The 2-thioxo- function of the starting materials **4-21** was then alkylated using 1-(chloromethyl)-4-methoxybenzene and potassium carbonate in dimethylformamide to afford the quinazolin-4(*3H*)-ones derivatives; 2-[(4-methoxybenzyl)-thio]-3-phenyl-6-methyl- (**22-27**), 2-[(4-methoxybenzyl)-thio]-3-phenyl-6-chloro- (**28-33**) and 2-[(4-methoxybenzyl)-thio]-3-phenyl-6,7-dimethoxy- (**34-39**). Compounds **4-21** were also reacted with 1-(chloromethyl)-3,4,5-trimethoxybenzene and potassium carbonate in dimethylformamide to afford 2-[(3,4,5-trimethoxybenzyl)-thio]-3-phenyl-6-methyl- (**40-45**), 2-[(3,4,5-trimethoxybenzyl)-thio]-3-phenyl-6-chloro- (**46-51**) and 2-[(3,4,5-tri-methoxybenzyl)-thio]-3-phenyl-6,7-dimethoxy- (**52-57**) -quinazolin-4(*3H*)-ones. The 2-thioxo-function of the starting materials **58-60** was then alkylated using 1-(chloromethyl)-4-methoxybenzene and potassium carbonate in dimethylformamide to afford 2-[(4-methoxy-benzyl)-thio]-3-benzyl-6-methyl- (**61**), 2-[(4-methoxy-benzyl)-thio]-3-benzyl-6-chloro- (**62**) and 2-[(4-methoxy-benzyl)-thio]-3-benzyl-6,7-dimethoxy- (**63**) quinazolin-4(*3H*)-one. Compounds **58-60** were also reacted with 1-(chloromethyl)-3,4,5-trimethoxybenzene and potassium carbonate in dimethylformamide to afford 2-[(3,4,5-trimethoxy-benzyl)-thio]-3-benzyl-6-methyl- (**64**), 2-[(3,4,5-trimethoxy-benzyl)-thio]-3-benzyl-6-chloro- (**65**) and 2-[(3,4,5-trimethoxy-benzyl)-thio]-3-benzyl-6,7-dimethoxy- (**66**) quinazolin-4(*3H*)-one. Structure elucidation of the synthesized products was attained by the aid of elementary analyses, ^{1}H & ^{13}C NMR spectroscopy, and mass spectrometry. The obtained data were in agreement with the desired structures. ^{1}H NMR spectrum of **22** showed three singlet absorptions at δ 1.42, 2.96, and 5.34 ppm attributed to the methyl, methoxy and methylene protons, respectively; in addition to the aromatic proton absorption which appeared in their expected range. Signals which observed at δ 37.5 and 172.6 in the ^{13}C NMR spectrum of **40** were correlated to methyl and carbonyl carbons. Further evidence for the formation of synthesized structures was attained by recording the mass spectra. The mass spectrum of compound **45** showed a molecular ion peak at m/z 462, which is in conformity with its molecular formula.

Scheme 1: Synthesis of the target compounds **22-57**

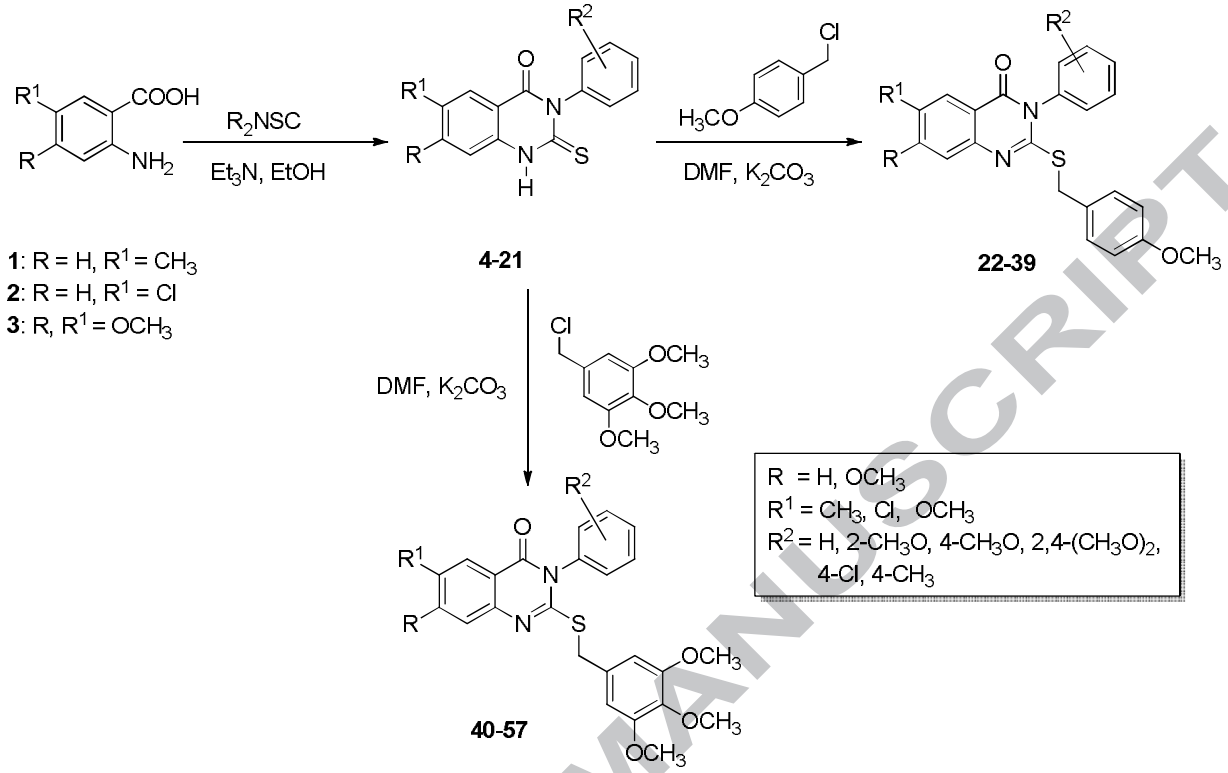

Scheme 2: Synthesis of the target compounds **61-66**

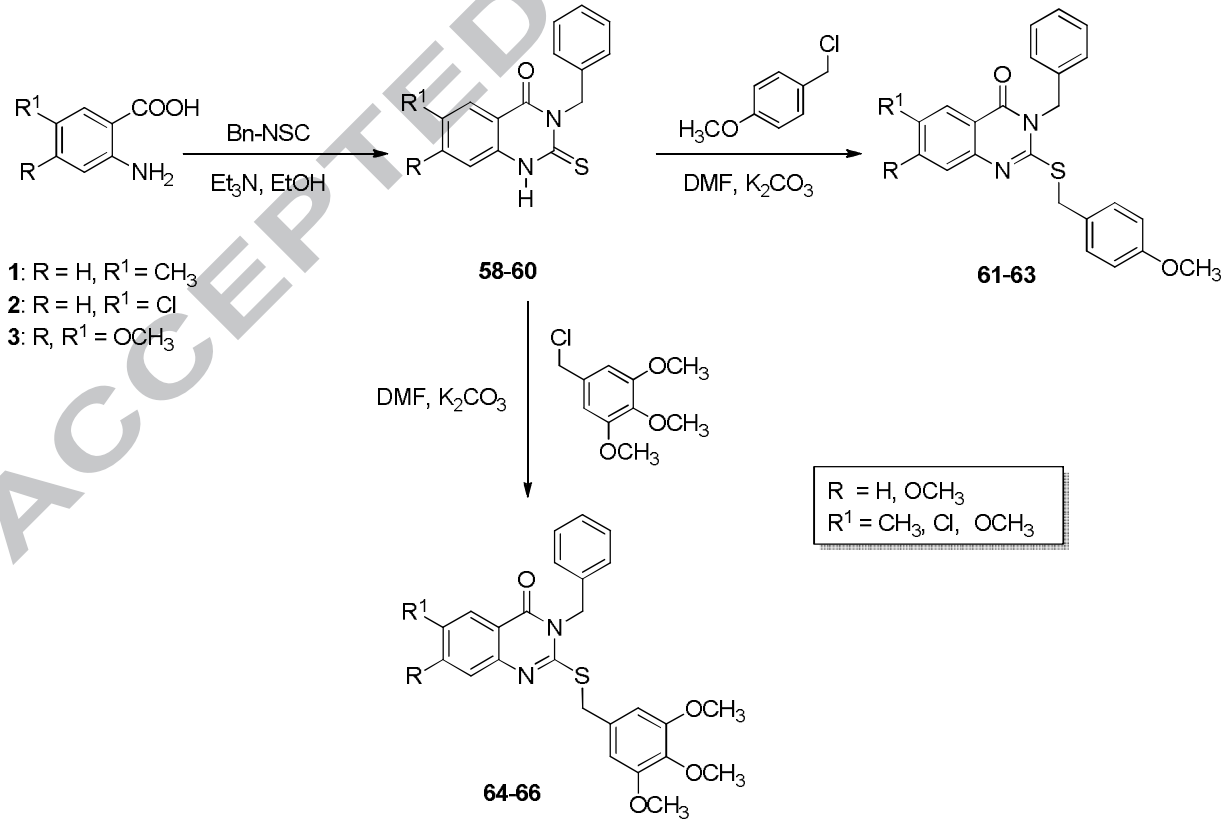

Table 1: Physicochemical properties and DHFR inhibition (IC_{50}, μM) of the synthesized compounds **22-57** and **61-66**

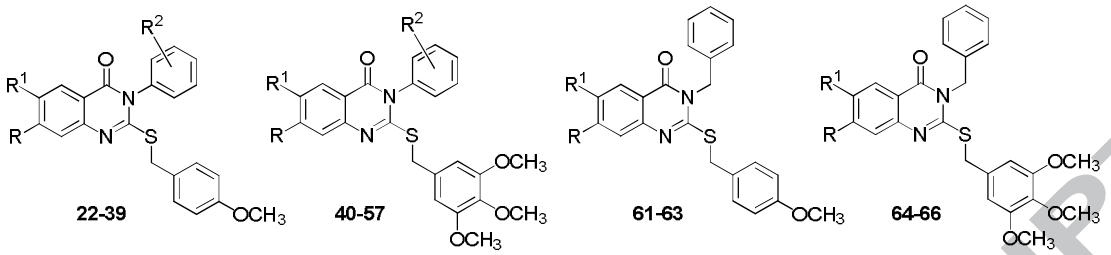

Compound	R	R^1	R^2	Yield %	M.p. °C	Molecular Formulae[a]	DHFR inhibition (IC_{50}, μM)
22	H	CH_3	H	58	170-172	$C_{23}H_{20}N_2O_2S$	0.1
23	H	CH_3	4-CH_3O	67	189-191	$C_{24}H_{22}N_2O_3S$	1.2
24	H	CH_3	2-CH_3O	58	123-125	$C_{24}H_{22}N_2O_3S$	0.9
25	H	CH_3	2,4-$(CH_3O)_2$	62	155-157	$C_{25}H_{24}N_2O_4S$	0.7
26	H	CH_3	4-Cl	73	148-150	$C_{23}H_{19}ClN_2O_2S$	0.1
27	H	CH_3	4-CH_3	46	132-134	$C_{24}H_{22}N_2O_2S$	1.0
28	H	Cl	H	56	115-117	$C_{22}H_{17}ClN_2O_2S$	0.02
29	H	Cl	4-CH_3O	65	190-192	$C_{23}H_{19}ClN_2O_3S$	0.1
30	H	Cl	2-CH_3O	75	137-139	$C_{23}H_{19}ClN_2O_3S$	0.8
31	H	Cl	2,4-$(CH_3O)_2$	78	129-131	$C_{24}H_{21}ClN_2O_4S$	1.0
32	H	Cl	4-Cl	62	177-179	$C_{22}H_{16}Cl_2N_2O_2S$	3.0
33	H	Cl	4-CH_3	69	202-204	$C_{23}H_{19}ClN_2O_2S$	4.0
34	CH_3O	CH_3O	H	55	178-180	$C_{24}H_{22}N_2O_4S$	4.0
35	CH_3O	CH_3O	4-CH_3O	53	211-213	$C_{25}H_{24}N_2O_5S$	0.8
36	CH_3O	CH_3O	2-CH_3O	58	244-246	$C_{25}H_{24}N_2O_5S$	0.6
37	CH_3O	CH_3O	2,4-$(CH_3O)_2$	67	138-140	$C_{26}H_{26}N_2O_6S$	0.3
38	CH_3O	CH_3O	4-Cl	79	166-168	$C_{24}H_{21}ClN_2O_4S$	6.0
39	CH_3O	CH_3O	4-CH_3	50	199-201	$C_{25}H_{24}N_2O_4S$	2.0
40	H	CH_3	H	67	152-154	$C_{25}H_{24}N_2O_4S$	7.0
41	H	CH_3	4-CH_3O	69	140-142	$C_{26}H_{26}N_2O_5S$	10.0
42	H	CH_3	2-CH_3O	55	214-216	$C_{26}H_{26}N_2O_5S$	1.0
43	H	CH_3	2,4-$(CH_3O)_2$	42	115-117	$C_{27}H_{28}N_2O_6S$	3.0
44	H	CH_3	4-Cl	59	252-254	$C_{25}H_{23}ClN_2O_4S$	0.9
45	H	CH_3	4-CH_3	69	166-168	$C_{26}H_{26}N_2O_4S$	1.5
46	H	Cl	H	54	138-140	$C_{24}H_{21}ClN_2O_4S$	0.8
47	H	Cl	4-CH_3O	59	94-96	$C_{25}H_{23}ClN_2O_5S$	3.0
48	H	Cl	2-CH_3O	56	188-190	$C_{25}H_{23}ClN_2O_5S$	0.1
49	H	Cl	2,4-$(CH_3O)_2$	58	167-169	$C_{26}H_{25}ClN_2O_6S$	4.0
50	H	Cl	4-Cl	50	188-190	$C_{24}H_{20}Cl_2N_2O_4S$	2.0
51	H	Cl	4-CH_3	65	191-193	$C_{25}H_{23}ClN_2O_4S$	3.0
52	CH_3O	CH_3O	H	70	155-157	$C_{26}H_{26}N_2O_6S$	0.9
53	CH_3O	CH_3O	4-CH_3O	68	195-195	$C_{27}H_{28}N_2O_7S$	1.2
54	CH_3O	CH_3O	2-CH_3O	63	232-234	$C_{27}H_{28}N_2O_7S$	0.8
55	CH_3O	CH_3O	2,4-$(CH_3O)_2$	65	211-213	$C_{28}H_{30}N_2O_8S$	3.0
56	CH_3O	CH_3O	4-Cl	77	215-217	$C_{26}H_{25}ClN_2O_6S$	0.9
57	CH_3O	CH_3O	4-CH_3	76	170-172	$C_{27}H_{28}N_2O_6S$	1.2
61	H	CH_3	-	49	110-112	$C_{24}H_{22}N_2O_2S$	0.01
62	H	Cl	-	58	149-151	$C_{23}H_{19}ClN_2O_2S$	1.1
63	CH_3O	CH_3O	-	58	189-191	$C_{25}H_{24}N_2O_4S$	0.8
64	H	CH_3	-	76	128-130	$C_{26}H_{26}N_2O_4S$	1.0
65	H	Cl	-	72	125-127	$C_{25}H_{23}ClN_2O_4S$	4.0
66	CH_3O	CH_3O	-	72	176-178	$C_{27}H_{28}N_2O_6S$	2.0

[a]Analysed for C,H,N,; results were within ± 0.4 % of the theoretical values for the given formulae.

The synthesized compounds (**22**-**57** and **61**-**66**) were evaluated as inhibitors of bovine liver DHFR using reported procedure [29]. Results were reported as IC_{50} values (Table 1). Compounds **28**, and **61** proved to be the most active DHFR inhibitors with IC_{50} values of 0.02 and 0.01 μM, respectively; while compounds **22**, **24**-**27**, **29**-**31**, **35**-**37**, **42**, **44**, **46**, **48**, **52**, **54**, **56**, **63** and **64** considered of moderate activity with IC_{50} range of 0.1-1.0 μM; compounds **23**, **39**, **45**, **50**, **53**, **57**, **62** and **66** showed weak activity with IC_{50} range of 1.1-2.0 μM. Methotrexate (IC_{50} 0.008 μM) was used as a positive control. Compounds **22**-**57** and **61**-**66** were further tested for their *in vitro* antimicrobial activity against a panel of standard strains of the *Gram-positive* bacteria (*Staphylococcus aureus* and *Bacillus subtilis*), the *Gram-negative* bacteria (*Escherichia coli* and *Pseudomonas aeuroginosa*), and the yeast-like pathogenic fungus *Candida albicans*. The primary screen was carried out using the agar disc-diffusion method using Müller-Hinton agar medium [30,31]P.

Table 2: Antimicrobial activity results of the tested compounds.

Compound	*S. aureus*	*B. subtilis*	*E. coli*	*P. aeuroginosa*	*C. albicans*
22	18 (4.0)	22 (2.0)	16 (8.0)	12	**-**
28	14	16	-	-	**-**
31	15 (8.0)	18 (4.0)	-	-	**-**
34	24 (2.0)	26 (2.0)	14 (8.0)	-	12
38	20 (4.0)	18 (4.0)	15 (8.0)	-	**-**
46	17 (8.0)	20 (4.0)	16 (8.0)	-	**-**
52	15 (8.0)	19 (8.0)	18 (8.0)	16 (8.0)	**-**
56	22 (4.0)	26 (2.0)	18 (8.0)	12	**-**
66	20 (4.0)	22 (4.0)	16 (8.0)	-	**-**
Gentamicin	26.5 (2.0)	25 (2.0)	20.8 (0.5)	19 (1.0)	Nd
Ciprofloxacin	32 (0.5)	35 (0.5)	38 (0.25)	36 (1.0)	Nd
Clotrimazole	Nd	Nd	Nd	Nd	21

Inhibition Zone (mm): (-) Not active (8 mm), Weak activity (8-12 mm), Moderate activity (12-15 mm), Strong activity (> 15 mm). Solvent: DMSO (8 mm). MICs showed in parentheses. Nd, not determined.

The results of the preliminary antimicrobial testing of the synthesized compounds are shown in Table 2. The majority of the synthesized compounds showed varying degrees of inhibition against the tested microorganisms. Compounds **22**, **28**, **31**, **34**, **38**, **46**, **52**, **56** and **66** proved moderate active against the Gram-positive bacteria *Staphylococcus aureus* and *Bacillus subtilis.* The inhibitory activity against the tested Gram-negative bacteria *Pseudomonas aeuroginosa* was lower than the other tested microorganisms. The minimal inhibitory concentration (MIC) for the most active compounds **22**, **31**, **34**, **38**, **46**, **52**, **56** and **66** was carried out using the micro-dilution susceptibility method in Müller-Hinton Broth; as shown in Table 2. It could be concluded that the Gram-positive bacteria *Bacillus subtilis* and to a lesser extent *Staphylococcus aureus* beside the Gram-negative bacteria *Escherichia coli* are sensitive to the tested compounds. In the present study, compounds **34**,

56 and **66** proved to be the most active broad spectrum antimicrobial agents against the used strains. Compounds **56** (IC_{50} 0.9 μM) and **66** (IC_{50} 2.0μM) might exert their antimicrobial activity through DHFR inhibition.

Compounds **22**-**57** and **61**-**66** were also subjected to the National Cancer Institute (NCI) *in vitro* antitumor activity. A single arbitrary dose (10 μM) of the test compounds were used in the full NCI 60 cell lines panel assay which includes nine tumor subpanels. The most active members of this study, compounds **40**, **41**, **43**, **48**, and **64**-**66** proved lethal to numerous cancer cell lines and passed the primary anticancer assay (Table 3). Consequently, those active compounds were carried over and tested against tumor cell lines at a 5-log dose range [25-28]. Three response parameters, GI_{50}, TGI, and LC_{50} were monitored for each cell line, using the known drug 5-Fluorouracil (5-FU) as a positive control. Compounds **40**, **41**, **43**, **48**, and **64**-**66** proved to be 2-10 fold more active than 5-FU, with GI_{50} MG-MID values of 2.2, 10.7, 4.3, 3.8, 2.4, 3.5 and 2.6 μM, respectively; detailed results are shown in Table 4. Compounds **64** (IC_{50} 1.0 μM) may exert its activity through DHFR inhibition.

Three groups of compounds synthesized differ in the type of the substituent at position 6- of the used quinazolines, namely, 6-methyl- (**22**-**27**, **40**-**45**, **61** and **64**), 6-chloro- (**28**-**33**, **46**-**51**, **62** and **65**), or 6,7-dimethoxy- (**34**-**39**, **52**-**57**, **63** and **66**) derivatives. The 2-thioether function affects the magnitude of DHFR inhibition. In the *3-phenyl series*, the 2-(4-methoxybenzyl)thio- function with order of activity 6-methyl- > 6-chloro- > 6,7-dimethoxy- (**22**-**39**) contributed to the DHFR inhibition activity more than 2-(3,4,5-trimethoxybenzyl)thio- group with order of activity 6-chloro- > 6,7-dimethoxy- > 6-methyl- (**40**-**57**). In the *3-benzyl series,* the 2-(4-methoxy-benzyl)thio- function (**61**-**63**) contributed to the DHFR inhibition activity more than 2-(3,4,5-trimethoxybenzyl)thio- group (**64**-**66**). In both groups, the order of activity was 6-methyl- > 6,7-dimethoxy- > 6-chloro-. In the *6-methyl series*, the combination of 3-phenyl- and 2-(4-methoxy-benzyl)thio- produced **22** with IC_{50} 0.1 μM; the introduction of 4-methoxy- or 4-methyl- groups to the 3-phenyl- function of **22** produced compounds with a pronounced decrease in activity; while the introduction of 4-chlorine atom preserved the DHFR inhibition potency of **22**. Replacing of the 2-(4-methoxy-benzyl)thio- moiety of **22** by 2-(3,4,5-trimethoxybenzyl)thio- function produced **40**-**45** with a remarkable decrease in potency. Replacing the 3-phenyl- of **22** by 3-benzyl- group produced one of the most active members of this study, compound **61** (IC_{50} 0.01 μM) with 10 fold increase in activity. In the *6-chloro series*, the presence of 3-phenyl- and 2-(4-methoxy-benzyl)thio- combination produced **28** with IC_{50} 0.02 μM. The *6,7-dimethoxy series*, showed the least active members of this investigation.

Table 3: Percentage growth inhibition (GI %) of *in vitro* subpanel tumor cell lines at 10 μM concentration of compounds **37**, **40**, **41**, **43**, **46**-**48**, **54**, **64**-**66**

Subpanel tumor cell lines	% Growth Inhibition (GI %)[a]										
	37	**40**	**41**	**43**	**46**	**47**	**48**	**54**	**64**	**65**	**66**
Leukemia											
HL-60(TB)	-	87.8	68.9	**L**	-	-	**L**	**L**	83.0	85.4	88.1
K-562	12.9	89.6	83.1	85.6	61.8	28.6	87.3	72.7	86.2	87.2	89.8
MOLT-4	20.6	78.2	44.0	88.7	30.3	27.6	84.7	53.2	69.2	70.6	83.3
RPMI-8226	36.3	45.1	-	**L**	-	33.8	82.6	28.8	46.0	31.3	45.3
SR	40.6	79.7	77.0	92.3	54.4	-	84.0	76.2	82.0	76.9	93.8
Non-small cell lung cancer											
A549/ATCC	19.2	60.7	49.0	81.1	26.1	20.2	68.9	12.0	60.0	57.8	63.2
HOP-62	-	62.2	34.8	52.6	28.0	-	48.2	-	60.0	62.3	58.6
HOP-92	24.5	32.1	-	77.3	11.1	42.9	57.1	34.2	43.4	28.7	37.4
NCI-H23	21.7	78.0	30.1	82.2	21.0	20.2	63.9	20.1	78.7	74.9	79.6
NCI-322M	19.4	52.6	19.7	72.0	14.3	-	44.9	14.9	53.8	52.5	54.6
NCI-H460	-	79.8	26.2	95.4	-	10.3	89.2	16.6	82.3	79.5	77.7
NCI-H522	31.4	91.7	60.7	-	61.6	16.7	-	-	**L**	**L**	**L**
Colon cancer											
COLO 205	-	**L**	67.3	**L**	15.5	-	72.0	-	**L**	**L**	92.6
HCC-2998	-	50.3	24.3	54.5	20.0	-	43.2	-	57.0	50.0	59.2
HCT-116	37.2	73.4	65.1	81.9	38.2	33.3	78.9	12.0	74.9	79.2	85.4
HCT-15	19.4	69.9	66.4	76.4	47.5	19.3	72.2	24.6	70.8	75.1	79.9
HT29	12.0	85.7	78.1	88.8	33.0	17.0	92.3	33.4	89.5	88.3	89.4
KM12	21.9	74.7	64.7	81.9	50.2	18.7	83.6	45.9	74.7	76.4	84.6
SW-620	-	70.3	50.7	27.9	20.3	-	83.2	23.6	74.2	71.4	66.6
CNS cancer											
SF-268	13.7	52.6	19.4	55.9	22.3	15.2	58.4	30.1	48.5	59.1	62.2
SF-295	10.4	67.2	48.6	93.7	15.8	16.7	68.2	26.2	69.0	71.1	80.3
SF-539	-	96.5	22.3	80.0	21.1	12.7	35.5	10.1	**L**	94.2	**L**
SNB-75	-	**L**	55.6	70.4	24.3	-	**L**	37.2	**L**	**L**	**L**
U251	-	61.5	30.9	75.2	11.4	-	74.5	13.2	67.0	67.2	71.0
Melanoma											
LOX IMVI	16.6	64.0	37.0	68.4	20.7	18.0	66.8	22.7	60.2	60.7	62.3
MALME-3M	17.4	57.6	40.4	74.5	23.5	-	67.1	37.0	70.0	61.2	78.1
M14	-	82.8	46.2	88.8	-	-	84.1	23.0	64.4	64.7	85.2
MDA-MB-435	38.0	**L**	**L**	**L**	75.6	12.4	**L**	100	**L**	98.2	**L**
SK-MEL-2	-	85.3	35.3	-	22.5	-	-	-	99.1	78.6	**L**
SK-MEL-28	-	47.9	26.0	59.2	-	-	50.7	21.1	48.0	56.3	60.8
SK-MEL-5	19.5	80.0	45.2	82.4	18.8	15.1	72.3	-	82.2	74.4	**L**
UACC-257	-	49.8	22.7	-	10.3	11.2	-	-	52.6	53.5	36.7
UACC-62	19.8	79.2	43.3	75.6	35.9	33.9	65.7	27.5	78.6	84.8	76.6
Ovarian cancer											
IGORV1	14.0	66.8	38.0	64.3	27.5	16.3	52.3	16.9	75.7	64.7	60.8
OVCAR-3	-	**L**	40.1	**L**	22.2	-	99.5	51.8	**L**	**L**	93.8
OVCAR-4	16.8	42.8	32.8	42.6	18.3	28.3	37.0	16.9	46.9	48.0	55.8
OVCAR-5	-	53.6	19.4	56.8	15.4	10.5	46.7	11.0	54.7	53.3	46.3
OVCAR-8	10.8	47.2	15.8	54.5	15.7	13.7	44.7	15.4	64.9	47.1	-
NCI/ADR-RES	20.5	82.2	54.2	98.6	24.5	10.7	79.8	37.1	87.3	86.1	**L**
SK-OV-3	-	86.4	26.3	54.7	-	-	40.6	-	76.1	75.7	70.2
Renal cancer											
786-0	-	62.4	15.9	70.4	10.7	-	49.0	-	53.2	56.6	63.3
A498	41.4	84.0	62.0	**L**	18.3	49.1	95.0	74.6	93.0	76.0	**L**
ACHN	-	55.3	33.3	55.1	21.1	16.4	55.8	11.5	53.3	59.7	60.8
CAKI-1	31.3	72.4	45.8	86.7	26.1	33.0	57.4	57.1	71.3	73.3	74.3
RXF 393	24.5	85.8	47.2	80.4	31.1	25.9	38.5	22.0	**L**	86.9	95.5
SN12C	-	63.0	17.8	54.8	24.0	18.3	29.7	-	60.0	61.5	58.8
UO-31	44.6	75.9	52.8	81.8	52.2	52.1	57.4	63.7	68.0	72.9	65.3
Prostate cancer											
PC-3	44.4	51.0	25.0	91.3	26.8	37.7	80.4	38.9	54.1	44.9	51.2
Breast cancer											
MCF7	16.9	80.1	75.2	84.6	23.1	15.6	84.4	23.0	82.0	85.7	89.9
MDA-MB-231/ATCC	24.6	62.1	40.3	55.2	37.0	36.8	44.3	22.6	55.6	61.2	64.0
HS 578T	13.3	71.8	22.3	93.3	-	13.9	60.4	39.2	79.3	69.5	73.3
BT-549	-	80.4	28.6	67.9	-	-	60.5	12.5	65.2	78.3	83.2
T-47D	24.4	71.8	32.2	66.9	29.1	23.9	56.1	11.4	65.9	66.1	64.1
MDA-MB-468	25.7	**L**	53.2	83.0	42.7	13.4	84.4	23.0	**L**	**L**	**L**

[a] -, GI < 10%; nt, not tested; L, compound proved lethal to the cancer cell line.

Table 4: Median growth (GI_{50}) and total growth (TGI) inhibitory concentrations, (μM) of *in vitro* subpanel tumor cell lines

Compound	Activity	Subpanel tumor cell lines[a] I	II	III	IV	V	VI	VII	VIII	IX	MG-MID[b]
40	GI_{50}	1.8	3.0	1.3	5.4	3.9	4.0	4.2	3.4	2.3	2.2
	TGI	c	87.0	86.3	60.9	82.2	84.6	76.9	b	84.3	6.2
	LC_{50}	c	c	c	c	c	c	c	c	c	c
41	GI_{50}	3.4	34.5	18.2	30.9	19.7	46.9	39.7	52.8	5.3	10.7
	TGI	90.2	c	c	c	89.4	b	88.1	c	91.4	89.1
	LC_{50}	c	c	c	c	c	c	c	c	c	c
43	GI_{50}	2.5	17.7	4.4	9.6	4.2	5.1	15.4	3.7	4.1	4.3
	TGI	56.2	96.5	87.4	84.6	77.4	86.7	92.5	c	84.9	66.1
	LC_{50}	c	c	c	c	89.9	c	c	c	c	95.5
48	GI_{50}	2.4	5.8	3.1	7.9	4.2	6.7	10.6	5.9	3.5	3.8
	TGI	86.5	c	c	63.1	91.7	87.9	93.5	c	84.8	83.2
	LC_{50}	c	c	c	c	c	c	c	c	c	c
64	GI_{50}	2.4	4.0	1.6	3.5	3.2	3.3	4.3	2.9	2.8	2.4
	TGI	85.2	65.9	76.1	46.7	58.4	57.6	61.4	60.2	47.5	40.7
	LC_{50}	c	98.2	87.1	81.9	c	92.7	97.9	c	c	93.3
65	GI_{50}	3.0	5.5	3.1	4.2	4.4	5.2	4.4	4.0	3.3	3.5
	TGI	87.9	66.5	86.3	49.8	55.2	75.6	52.3	c	59.1	47.9
	LC_{50}	c	97.6	87.5	81.8	98.9	c	96.5	c	c	93.3
66	GI_{50}	1.9	3.6	2.2	3.4	2.6	6.4	4.7	4.0	2.5	2.6
	TGI	c	63.1	87.8	24.5	45.9	62.7	49.1	c	47.4	38.9
	LC_{50}	c	94.5	c	80.6	78.7	c	85.7	c	99.3	87.1
5-FU	GI_{50}	15.1	c	8.4	72.1	70.6	61.4	45.6	22.7	76.4	22.6
	TGI	c	c	c	c	c	c	c	c	c	c
	LC_{50}	c	c	c	c	c	c	c	c	c	c

[a]I, leukemia; II, non-small cell lung cancer; III, colon cancer; IV, CNS cancer; V, melanoma; VI, ovarian cancer; VII, renal cancer; VIII, prostate cancer; IX, breast cancer. [b]Full panel mean-graph midpoint (μM), [c] Compounds showed values > 100 μM.

The pattern of structure-activity variation in the 6-chloro- and 6,7-dimethoxy- derivatives is more or less similar to what has been noticed in the 6-methyl- series. In general, the type of substituent at positions 2-, 3-, and 6- of the quinazoline nucleus proved to manipulate and contribute to the DHFR inhibition activity. The antitumor activity was confined to the 2-(3,4,5-trimethoxy-benzyl)thio- rather than the 2-(4-methoxybenzyl)thio- analogues. In the *3-phenyl series*, the 6-methyl- derivative **40** proved to be the most active member with GI_{50} value of 2.2 μM. The introduction of 2- or 4-methoxy- group to the 3-phenyl function of **40** decreased the antitumor potency as shown in **41** and **43** with GI_{50} values of 10.7 and 4.3 μM, respectively; replacing the 6-methyl- by 6-chloro- regained some of the potency (**48**, GI_{50} 3.8 μM). In the *3-benzyl series,* the 6-methyl derivative **64** exhibited GI_{50} value of 2.4 μM. Replacing the 6-methyl- of **64** by 6-chloro- moiety produced **65** with a decreased potency (GI_{50} 3.5 μM); while the introduction of 6,7-dimethoxy- yielded **66** (GI_{50} 2.6 μM)

and helped to regain some of the activity of **64** .

The inhibitory activity of the new synthesized against DHFR was experimentally determined. Compounds **28** and **61** proved to be the active members in the present study (IC_{50} 0.02 and 0.01 µM, respectively) compared to the positive control MTX (IC_{50}, 0.008 µM). Molecular modeling study was necessary to obtain the binding mode in addition to get a consistent, more precise picture of the biologically active molecules at the atomic level and furthermore, to clarify the reasons behind diminished activity of the inactive candidates. A comparative modeling study of the active DHFR inhibitor **61** (IC_{50}, 0.01 µM) and the least active compound **41** (IC_{50}, 10 µM), against MTX was performed. The tertiary complex of human dihydrofolate reductase (hDHFR) crystal structure (pdb ID: 1DLS obtained from the protein data bank), NADPH and MTX were used as reference for modeling and docking [32]. Conformational search of initial structures of the selected molecules were constructed using MOE. The MM (calculations *in vacuo*, bond dipole option for and RMSD gradient of 0.01 kcal/mol) energy minima were determined by a semi-empirical method AM1 (as implemented). The energy-minimized geometry was used for the docking calculation and the various 2D descriptors using molecular modeling software MOE 2009.10 [33]. An analysis of the respective docking pose of active DHFR inhibitor compound **61** shows high affinity binding energy of -13.1387 Kcal/mol (even higher than MTX -12.9876 Kcal/mol) with Phe34 amino acid *via* arene-arene interaction (Figure 2) while the inactive compound **41** shows no binding with any amino acid residue in DHFR binding pocket (Figure 3) with less binding affinity energy of -11.3412 Kcal/mol. Each compound has its own unique feature of binding profile which could explain their different patterns in DHFR inhibitory activity regardless of their similarity in chemical structure.

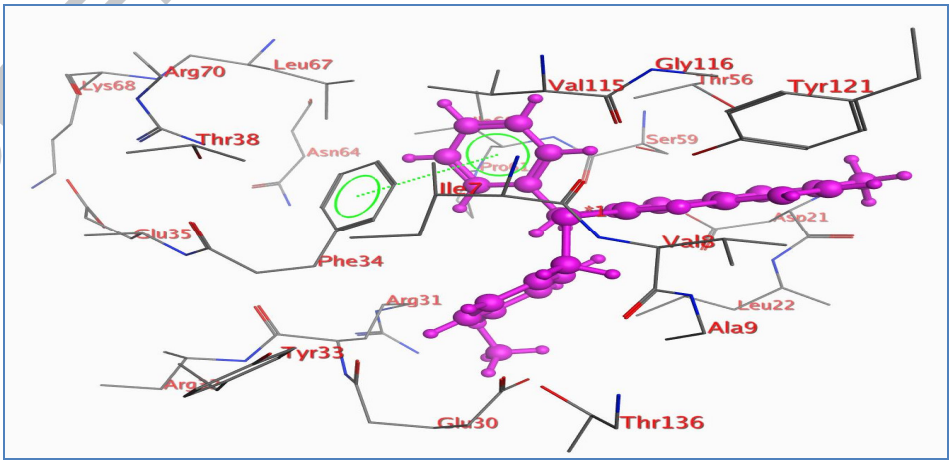

Figure 2: 3D binding mode and residues involved in the recognition for the most active compound **61** (IC_{50} 0.01 µM).

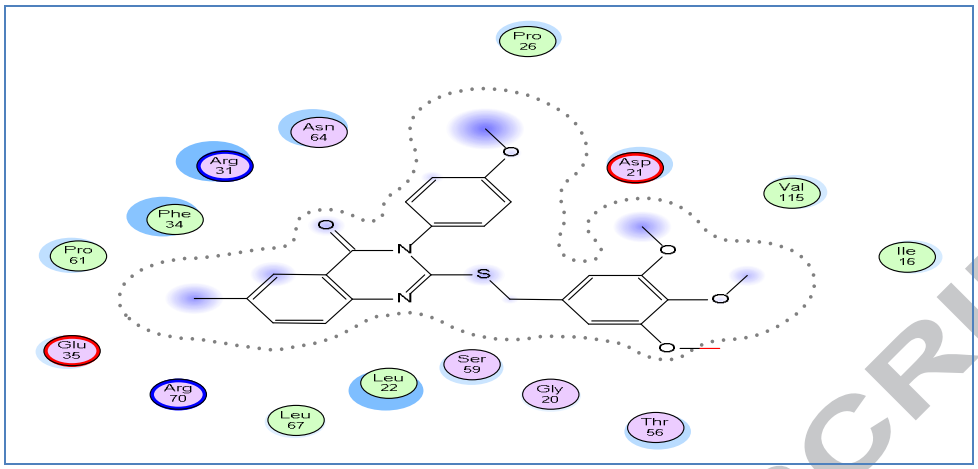

Figure 3: 2D binding mode and residues involved in the recognition and the least active compound **41** (IC_{50} 10.0 µM) docked and minimized in the DHFR binding pocket.

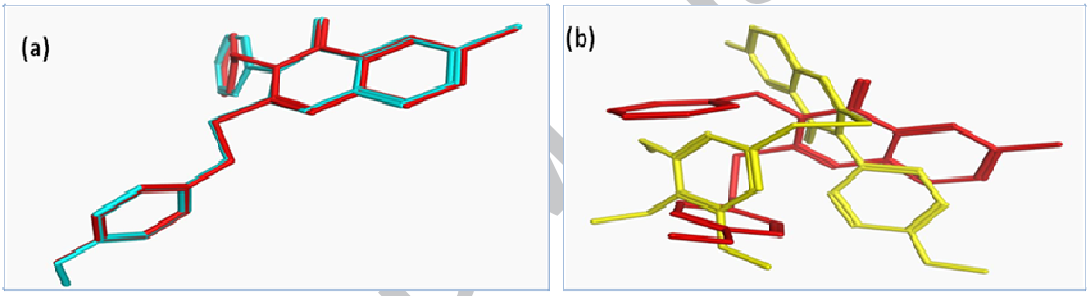

Figure 4: (a) Flexible alignment of the most active compounds and **61** (red), IC_{50} 0.01 µM and **28** (cyan), IC_{50} 0.02 µM. (b) Flexible alignment of the most active compound **61** (red), IC_{50} 0.01 µM and the least active compound **41** (yellow), IC_{50} 10.0 µM.

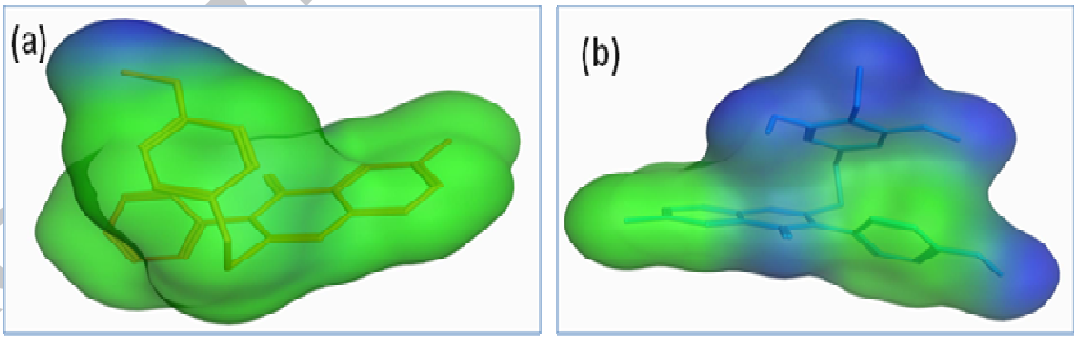

Figure 5: (a) Surface map for the most active compound **61** (orange) in pocket side. (b) Surface map for the least active compound **41** (cyan) in pocket side. Pink: hydrophilic, blue: mild polar, green: hydrophobic.

Flexible alignment technique [34] was performed using MOE/MMFF94 to automatically produce superposition of the compounds under investigation with minimal user bias. 200 conformers of each

compound were generated then minimized by a distance-dielectric dependent model. To investigate the similarity between the 3D structures of the most active compounds **61** (IC_{50}, 0.01 μM) and **28** (IC_{50}, 0.02 μM) as selected examples, flexible alignment was employed where it was clear that both compounds have shown good alignment profile (Figure 4a). On the contrary, Figure 4b obviously indicated a different alignment profiles for compounds **61** (IC_{50}, 0.01 μM) and **41** (IC_{50}, 10.0 μM). These findings are consistent with the obtained DHFR inhibition experimental data. To study the reasons for the decreased DHFR inhibition potency of **41** hydrophobic surface mapping studies were conducted. Compound **61** showed more intense greener hydrophobic distributions which could be responsible for the interaction with amino acid residues inside the enzyme active pocket (Figure 5a). On the other hand, the hydrophobic regions of the least active compound **41** seemed to be more near to the mild polar blue side (Figure 5b), hence the required lipophilicity for the effective binding to DHFR could be decreased. The performed molecular modeling studies with proposed binding mode analysis for **61** revealed some features which could embrace the importance of hydrophobicity and aromatic π-systems as crucial criteria required for interaction with the active site.

In Conclusion, compounds **28** and **61** proved to be the most active DHFR inhibitors with IC_{50} 0.02 and 0.01 μM, respectively. Structure activity relationship revealed that, the type of substituent at positions 2-, 3- and 6- of the studied quinazolin-4-ones manipulate the DHFR inhibition activity. The order of activity in the 2-(4-methoxybenzyl)thio- derivatives was 6-methyl- > 6-chloro- > 6,7-dimethoxy-; while in case of the 2-(3,4,5-trimethoxybenzyl)thio- was 6-chloro- > 6,7-dimethoxy- > 6-methyl-. Compounds **34**, **56** and **66** showed remarkable broad spectrum antimicrobial activity against both Gram-positive and Gram-negative bacteria comparable to the known antibiotics Gentamicin and Ciprofloxacin. Compounds **56** (IC_{50} 0.9 μM) and **66** (IC_{50} 2.0μM) may exert their activity through DHFR inhibition. Meanwhile, Compounds **40** and **64** showed broad spectrum antitumor activity toward several tumor cell lines and proved to be 10 fold more active than 5-FU, with GI_{50} MG-MID 2.2 and 2.4 μM, respectively. Compound **64** (IC_{50} 1.0 μM) might exert its activity through DHFR inhibition. Molecular modeling studies concluded that recognition with key amino acid Phe34 is essential for binding and DHFR inhibition. The binding mode for the most active compound **61** at the active site of hDHFR was consistent with the experimental data. Analysis of this binding mode emphasis the common features highlighting the importance of hydrophobicity and aromatic π-systems in binding to the DHFR active site. Figure 6 showed the structures of the most active DHFR inhibitors **28** and **61**; the broad spectrum antibacterial **34**; in addition to the antitumor agents **40**, **64**.

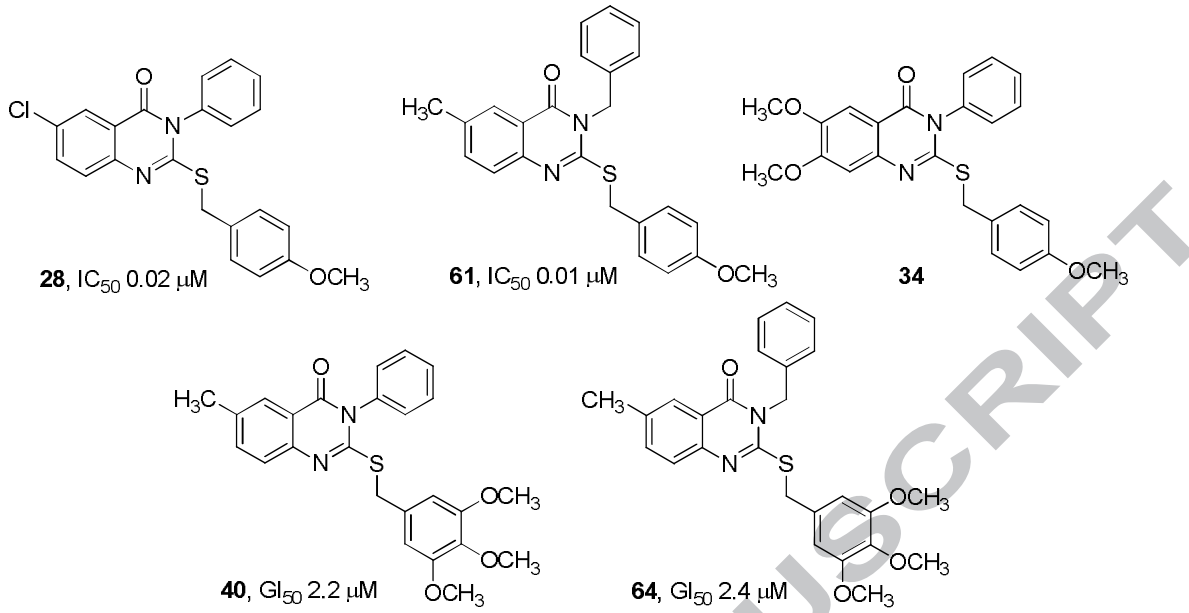

Figure 6: Structures of the most active DHFR inhibitors **28**, **61**; the broad spectrum antibacterial **34**; and the antitumor agents **40**, **64**.

Comparing the obtained results to that for the leads **A**-**C** (Figure 1, IC_{50} range of 0.3-1.0 μM), clearly shows that the introduction of methoxylated 2-(arylmethyl-thio)- as hydrophobic π-system regions to the used quinazolines (compounds **61** and **28**, IC_{50} 0.01 and 0.02 μM, respectively) confirmed the feasiblity of the reported pharmacophoric features mentioned in the introduction and hence contributed with positive impact to the DHFR inhibition activity. The methoxylated 2-(arylmethyl-thio)-function containing compounds proved to be 30-100 fold more active than the 2-allylthio-, 2-thiazolylthio- or 2-thiadiazolylthio- groups shown in **A**-**C**. The obtained model could be useful for further development of new DHFR inhibitors.

Acknowledgements

Thanks are due to the NCI, Bethesda, MD, for performing the antitumor testing of the synthesized compounds

References and Notes

1. Masur, H. *J. Infect. Dis.* **1990**, *161*, 858–864.

2. Berman, E.M.; Werbel, L.M. *J. Med. Chem.* **1991**, *34*, 479-485.

3. Borst, P.; Quellette, M. *Annu. Rev. Microbiol*. **1995**, *49*, 427-460.

4. Hassan, G.S.; El-Messery, S.M.; Al-Omary, F.A.M.; El-Subbagh, H.I. *Bioorg. & Med. Chem. lett.* **2012**, *22*, 6318–6323.

5. El-Messery, S.M.; Hassan, G.S.; Al-Omary, F.A.M.; El-Subbagh, H.I. *Eur. J. Med. Chem.* **2012**, *54*, 615-625.

6. Abdel-Aziz, A.A.-M.; El-Azab, A.S.; El-Subbagh, H.I.; Al-Obaid, A.M.; Alanazi, A.M.; Al-Omar, M.A. *Bioorg. & Med. Chem. lett.* **2012**, *22*, 2008-2014.

7. Taher, A.T.; Georgey, H.H.; El-Subbagh, H.I. *Eur. J. Med. Chem.* **2012**, *47*, 445-451.

8. Al-Omary, F.A.M.; Hassan, G.S.; El-Messery, S.M.; El-Subbagh, H.I. *Eur. J. Med. Chem.* **2012**, *47*, 65-72.

9. El-Subbagh, H.I.; Abadi, A.H.; Al-Khamees, H.A. *Arch. Pharm. Pharm. Med. Chem.* **1997**, *330*, 277–282.

10. El-Subbagh, H.I.; Abadi, A.H.; El-Khawad, I.E.; Rashood, K.A. *Arch. Pharm. Pharm. Med. Chem.* **1999**, *332*, 19–22.

11. El-Subbagh, H.I.; Abu-Zaid, S.M.; Mahran, M.A.; Badria, F.A.; Al-Obaid, A.M. *J. Med. Chem.* **2000**, *43*, 2915-2921.

12. Al-Madi, S.H.; Al-Obaid, A.M.; El-Subbagh, H.I. *Anticancer Drugs* **2001**, *12* 835-841.

13. Abdel Hamid, S.G.; El-Obaid, H.A.; Al-Rashood, K.A.; Khalil, A.A.; El-Subbagh, H.I. *Sci. Pharm*. **2001**, *69*, 351–366.

14. Khalil, A.A.; Abdel Hamide, S.G.; Al-Obaid, A.M.; El–Subbagh, H.I. *Arch. Pharm. Pharm. Med. Chem.* **2003**, *336*, 95–103.

15. Abdel Hamid, S.G.; El-Obaid, H.A.; Al-Majed, A.A.; El-Kashef, H.A.; El-Subbagh, H.I. *Med. Chem. Res*. **2001**, *10*, 378–389.

16. Al-Omar, M.A.; Abdel Hamide, S.G.; Al-Khamees, H.A.; El-Subbagh, H.I. *Saudi Pharm. J.* **2004**, 12, 63-71.

17. Al-Rashood, S.T.; Aboldahab, I.A.; Abouzeid, L.A.; Abdel-Aziz, A.A-M.; Nagi, M.N.; Abdulhamide, S.G.;Youssef, K.M.; Al-Obaid, A.M.; El-Subbagh, H I. *Bioorg. & Med. Chem.* **2006**, *14,* 8608-8621.

18. Al-Omary, F. A. M.; Abou-zeid, L.A.; Nagi, M.N.; Habib, E. E.; Abdel-Aziz, A. A.-M.; El-Azab, A.S.; Abdel-Hamide, S. G.; Al-Omar, M. A.; Al-Obaid, A. M.; El-Subbagh, H. I. *Bioorg. & Med. Chem*. **2010**, *18*, 2849-2863.

19. Al-Omary, F.A.M.; Hassan, G.S; El-Messery, S.M.; Nagi, M.N.; Habib, E.E.; El-Subbagh, H.I. *Eur. J. Med. Chem.* **2013**, *63*, 33-45.

20. Hassan, G.S.; El-Messery, S.M.; Al-Omary, F.A.M.; Al-Rashood, S.T.; Shabayek, M.I.; Abulfadl, Y.S.; Habib, E.E.; El-Hallouty, S.M.; Fayad, W.; Mohamed, K.M.; El-Menshawi, B.S.; El-Subbagh H.I. *Eur. J. Med. Chem*. **2013**, *66*, 135-145.

21. El-Subbagh, H.I.; Hassan, G.S.; El-Messery, S.M.; Al-Omary, F.A.M.; Al-Rashood, S.T.; Abulfadl, Y.S.; Shabayek, M.I. *Eur. J. Med. Chem.* **2014**, 74, 234-245.

22. Al-Rashood, S.T.; Hassan, G.S.; El-Messery, S.M.; Nagi, M.N.; Habib, E.E.; Al-Omary, F.A.M.; El-Subbagh, H.I. *Bioorg. & Med. Chem. Lett.* **2014**, *24*, 4557–4567.

23. Foye, W.O.; Lemke, T.L.; Williams, D.A. *Principles of Medicinal Chemistry 4th Ed.,* Williams and Wilkins: Media, PA, **2005** 442-456.

24. Nordberg, M.G.; Kolmodin, K.; Aqvist, J.; Queener, S.F.; Hallberg, P. *Eur. J. Pharm. Sci.* **2004**, *22*, 43–53.

25. Grever, M.R.; Schepartz, S.A.; Chabner, B.A. *Semin. Oncol.* **1992**, *19*, 622–638.

26. Monks, A.; Scudiero, D.; Skehan, P. *J. Natl. Cancer. Inst*. **1991**, *83* 757–766.

27. Boyd, M.R.; Paull, K.D. *Drug Rev. Res*. **1995**, *34*, 91–109.

28. Skehan, P.; Storeng, R.; Scudiero, D.; Monks, A.; McMahon, J.; Vistica, D. Warren, J.R. ; Bokesch, H.; Kenney, S.; Boyd, M.R. *J. Natl. Cancer Inst*. **1990**, *82*, 1107−1112.

29. Pignatello, R.; Sapmpinato, G.; Sorrenti, V.; Vicari, L.; Di-Giacomo, C.; Vanella, A.; Puglisi, G. *Pharm. Pharmacol. Commun*. **1999**, *5*, 299−504.

30. Clinical and Laboratory Standards Institute (CLSI). Performance standards for antimicrobial susceptibility testing, CLSI approved standards M100-S15., Wayne, PA, 2008.

31. Murray, P. R.; Baron, E. J.; Pfaller, M. A.; Tenover, F. C.; Yolken, R. H. *In Manual of Clinical Microbiology*; Wood, G. L.; Washington, J. A., Eds. *Am. Soc. Microbiol*.: Washington D.C.1995

32. Lewis, W.S.; Cody, V.; Galitsky, N.; Luft, J.R.; Pangborn, W.; Chunduru, S.K.; Spencer, H.T.; Appleman, J.R.; Blakley, R.L. *J. Biol. Chem.* **1995**, *270*, 5057-5064.

33. Molecular Operating Environment (MOE), **2009**.10; Chemical Computing Group Inc.

34. Cody, V.; Schwalbe, C.H. *Crystallography Reviews* **2006**, *12*, 301–333.

35. Profeta, S.; Allinger. N. L. *J. Am. Chem. Soc*. **1985**, *107*, 1907-1918.

36. Allinger. N. L. *J. Am. Chem. Soc*. **1977**, 99, 8127-8134.

37. Labute, P.; Williams, C.; Feher, M.; Sourial, E.; Schmidt, J.M. *J. Med. Chem.* **2001**, *44*, 1483–1490.

38. Kearsley, S.; Smith, G.M. *Tetrahedron Comput. Methodol*. **1990**, *3*, 615–633.

Graphical Abstract

Synthesis, biological evaluation and molecular modeling study of some new methoxylated 2-benzylthio-quinazoline-4(3H)-ones as nonclassical antifolates.

Shahenda M. El-Messery,[a*] Ghada S. Hassan,[b] Mahmoud N. Nagi,[c] El-Sayed E. Habib,[d,e] Sarah T. Al-Rashood,[f] Hussein I. El-Subbagh.[b,g*]

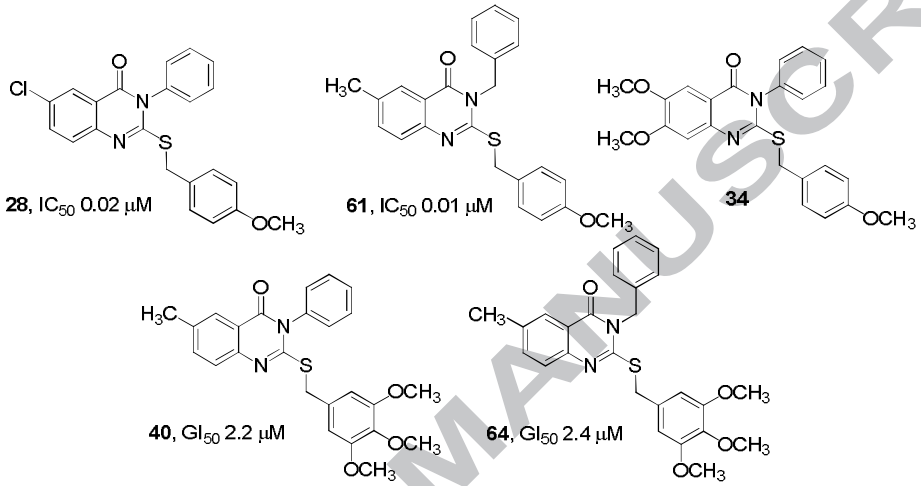

The DHFR inhibitors **28**, **61**; the broad spectrum antibacterial **34**; and the antitumor agents **40**, **64**.

39.